Proc. Natl. Acad. Sci. USA
Vol. 93, pp. 10489–10494, September 1996
Pharmacology

NO hyperpolarizes pulmonary artery smooth muscle cells and decreases the intracellular Ca^{2+} concentration by activating voltage-gated K^+ channels

(potassium current/membrane potential/4-aminopyridine/nitroprusside)

XIAO-JIAN YUAN*, MARY L. TOD, LEWIS J. RUBIN, AND MORDECAI P. BLAUSTEIN

Division of Pulmonary and Critical Care Medicine, Departments of Medicine, Physiology, and Pediatrics, University of Maryland School of Medicine, Baltimore, MD 21201

Communicated by Robert F. Furchgott, State University of New York Health Science Center, Brooklyn, NY, May 28, 1996 (received for review December 18, 1995)

ABSTRACT **NO causes pulmonary vasodilation in patients with pulmonary hypertension. In pulmonary arterial smooth muscle cells, the activity of voltage-gated K^+ (K_V) channels controls resting membrane potential. In turn, membrane potential is an important regulator of the intracellular free calcium concentration ($[Ca^{2+}]_i$) and pulmonary vascular tone. We used patch clamp methods to determine whether the NO-induced pulmonary vasodilation is mediated by activation of K_V channels. Quantitative fluorescence microscopy was employed to test the effect of NO on the depolarization-induced rise in $[Ca^{2+}]_i$. Blockade of K_V channels by 4-aminopyridine (5 mM) depolarized pulmonary artery myocytes to threshold for initiation of Ca^{2+} action potentials, and thereby increased $[Ca^{2+}]_i$. NO ($\approx$3 μM) and the NO-generating compound sodium nitroprusside (5–10 μM) opened K_V channels in rat pulmonary artery smooth muscle cells. The enhanced K^+ currents then hyperpolarized the cells, and blocked Ca^{2+}-dependent action potentials, thereby preventing the evoked increases in $[Ca^{2+}]_i$. Nitroprusside also increased the probability of K_V channel opening in excised, outside-out membrane patches. This raises the possibility that NO may act either directly on the channel protein or on a closely associated molecule rather than via soluble guanylate cyclase. In isolated pulmonary arteries, 4-aminopyridine significantly inhibited NO-induced relaxation. We conclude that NO promotes the opening of K_V channels in pulmonary arterial smooth muscle cells. The resulting membrane hyperpolarization, which lowers $[Ca^{2+}]_i$, is apparently one of the mechanisms by which NO induces pulmonary vasodilation.**

Endothelium-derived relaxing factor, which was first described by Furchgott and Zawadzki in 1980 (1), plays an important role in controlling vascular tone. NO, the best characterized endothelium-derived relaxing factor (2, 3), can be produced by both vascular endothelium and smooth muscle cells (4). Basal release of endothelium-derived NO may help to maintain low resting pulmonary vascular tone in normal humans (4, 5). Dysfunction of endothelial NO production and release is believed to be a major cause of pulmonary hypertension and its sequelae (6, 7). Inhaled NO selectively causes pulmonary vasodilation in patients with pulmonary hypertension (8, 9).

The cellular mechanisms of NO-induced pulmonary vasodilation are not completely understood. They apparently involve an increase of intracellular cGMP (10, 11) as well as membrane hyperpolarization (12, 13). The activity of sarcolemmal voltage-gated K^+ (K_V) channels controls the resting membrane potential (E_m), which is, in turn, an important regulator of the intracellular free Ca^{2+} concentration ($[Ca^{2+}]_i$) (14, 15). Changes in $[Ca^{2+}]_i$ in pulmonary arterial smooth muscle cells (PASMC) play a critical role in regulating pulmonary vasomotor tone.

In PASMC, inhibition of K_V channels, for example by 4-aminopyridine (4-AP) (15, 16, 17), causes membrane depolarization. The depolarization opens voltage-gated Ca^{2+} channels and thereby initiates Ca^{2+}-dependent action potentials and raises $[Ca^{2+}]_i$ (15). The rise in $[Ca^{2+}]_i$ triggers contraction. Inhibition of Ca^{2+}-activated K^+ (K_{Ca}) channels by charybdotoxin (ChTX) and ATP-sensitive K^+ (K_{ATP}) channels by glibenclamide (15, 16), however, has no such effect on E_m and $[Ca^{2+}]_i$ under resting conditions. In contrast, hypoxia selectively inhibits K_V channels and thereby depolarizes PASMC (18–22). The resulting increase in $[Ca^{2+}]_i$ triggers pulmonary vasoconstriction (21, 23). Thus, the K_V channels may play a critical role in regulating E_m (15–17, 22, 24), $[Ca^{2+}]_i$ (15), and pulmonary vascular tone under resting physiological conditions.

Removal of the endothelium in isolated pulmonary artery (PA) rings significantly enhances hypoxia- and agonist-induced pulmonary vasoconstriction (23). This result raises the possibility that endothelium-derived NO influences $[Ca^{2+}]_i$ and pulmonary vascular tone by an action on PASMC K_V channels, although an effect of NO on the K_V channels has not previously been reported. This study was therefore undertaken to determine the effects of NO on K_V channel activity, E_m, and $[Ca^{2+}]_i$ in PASMC. Patch clamp techniques and quantitative fluorescence microscopy were used to identify the sequence of events involved in NO-mediated modulation of pulmonary arterial tone.

MATERIALS AND METHODS

Cell Preparation. Rat PASMC primary cultured for 3–7 days were used for this study. Details of the methods used for isolation and culture of PASMC are published (25). Briefly, the intrapulmonary arterial branches (3rd and 4th order) as well as the right and left branches (2nd order) of rat main PA were incubated for 20 min in Hanks' balanced salt solution containing collagenase (1.5 mg/ml; Worthington). Adventitia and endothelium were removed after incubation. The PA smooth muscle was then digested with 1.5 mg/ml collagenase, 0.5 mg/ml elastase (Sigma), and 1 mg/ml bovine albumin (Sigma) at 37°C to create a suspension of single PASMC. The cells were resuspended and plated onto 25-mm coverslips and

The publication costs of this article were defrayed in part by page charge payment. This article must therefore be hereby marked "*advertisement*" in accordance with 18 U.S.C. §1734 solely to indicate this fact.

Abbreviations: K_V channels, voltage-gated K^+ channels; $[Ca^{2+}]_i$, intracellular free calcium concentration; E_m, membrane potential; PASMC, pulmonary artery smooth muscle cells; 4-AP, 4-aminopyridine; K_{Ca} channels, Ca^{2+}-activated K^+ channels; ChTX, charybdotoxin; K_{ATP} channels, ATP-sensitive K^+ channels; PA, pulmonary artery; I_K, K^+ current; PSS, physiological salt solution; SNP, sodium nitroprusside; TEA, tetraethylammonium; *I–V*, current–voltage relationship; $N \times P_{open}$, steady-state open probability.

*To whom reprint requests should be addressed at: Division of Pulmonary and Critical Care Medicine, University of Maryland School of Medicine, 10 South Pine Street, Suite 800, Baltimore, MD 21201. e-mail: xyuan@umabnet.ab.umd.edu.

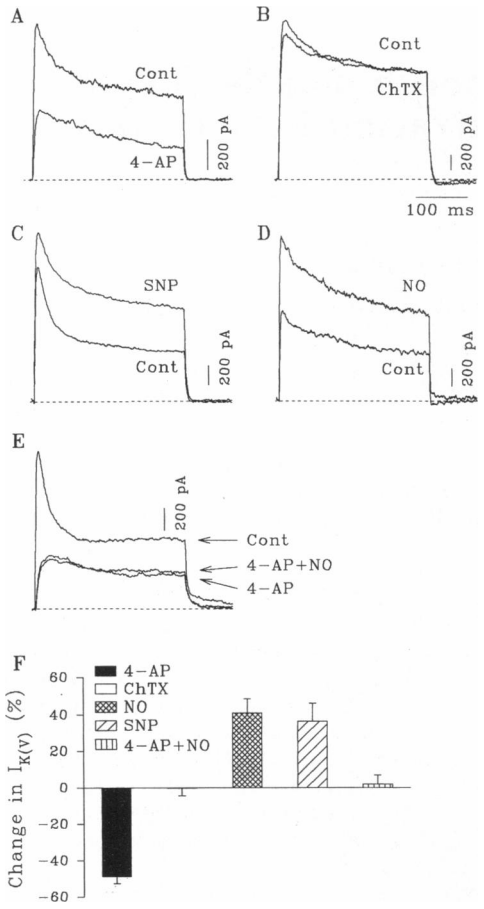

FIG. 1. Effects of 4-AP, ChTX, SNP, and authentic NO on whole-cell $I_{K(V)}$ in PASMC. Representative $I_{K(V)}$, elicited by depolarizing (300 msec) the cells from a holding potential of −70 mV to +80 mV, were recorded before (Cont) and during application of 5 mM 4-AP (*A*), 20 nM ChTX (*B*), 10 μM SNP (*C*), or ≈3 μM NO (*D*). (*E*) $I_{K(V)}$, elicited by a 300-msec test pulse of +80 mV, was recorded before (Cont) and during application of 4-AP in the absence (4-AP) or presence (4-AP+NO) of NO. Cells were superfused and dialyzed with the Ca^{2+}-free bath (with 1 mM EGTA) and pipette (with 10 mM EGTA) solutions. (*F*) Summarized data showing the effects of 4-AP (solid bar; n = 6), ChTX (open bar; n = 11), NO (crosshatched bar; n = 5), and SNP (hatched bar; n = 7) on the steady-state $I_{K(V)}$ (measured at 285–290 msec), and the effect of NO on $I_{K(V)}$ in the presence of 4-AP (vertical bar; n = 7). Values are means ± SE of percentage changes produced by 4-AP, ChTX, NO, and SNP on steady-state $I_{K(V)}$ evoked at +80 mV.

incubated in a humidified atmosphere of 5% CO_2/95% air at 37°C in 10% fetal bovine serum culture medium. Before each experiment (12–24 hr), the serum concentration in the medium was decreased to 0.3% to stop cell proliferation.

Recording of Whole-Cell and Single-Channel K^+ Currents. K^+ currents (I_K) were measured with an Axopatch-1D amplifier and PCLAMP software (Axon Instruments, Foster City, CA) using the patch clamp technique (26). Patch pipettes (2–4 MΩ) were fabricated from microhematocrit tubes (VWR Scientific) and were fire-polished on a microforge. Step-pulse protocols and data acquisition were performed by a TL-1 digital interface (Axon Instruments) coupled to an IBM-compatible computer. Whole-cell currents were filtered at 1–2 kHz (−3 dB) and digitized at 4–6 kHz using the amplifier and were recorded on a computer for offline analysis later. Series resistance and whole-cell capacitance were routinely compensated (40–70%) by adjusting the internal circuitry of the patch clamp amplifier. Leakage currents were subtracted using the P/4 protocol in PCLAMP software.

In experiments with outside-out and cell-attached patches, a gigaohm seal was achieved using fire-polished glass electrodes

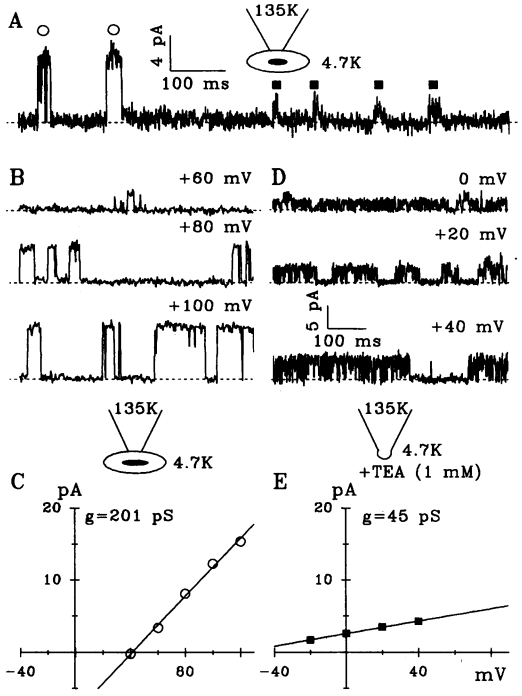

FIG. 2. Single-channel I_K recorded from cell-attached and outside-out membrane patches of PASMC. (*A*) Current trace from a cell-attached patch exposed to a symmetrical K^+ gradient (135 mM K^+). Patch command potential was held at +70 mV (the actual patch potential was about +30 mV since the average E_m is −40 mV). A larger amplitude current (○) and a smaller amplitude current (■) were observed upon depolarization. (*B*) Single-channel currents in the absence of TEA. The records show larger amplitude single-channel currents from a cell-attached PASMC membrane patch exposed to a symmetrical K^+ gradient. The membrane patch was held at +60, +80, and +100 mV, as indicated (the actual patch potential should be +20, +40, and +60 mV, respectively). Current levels when channels are closed are indicated by horizontal broken lines. Upward deflection represents outward current. (*C*) Single-channel current–voltage (*I–V*) curve for data from the large amplitude currents. The slope conductance (g) calculated from the *I–V* curve was 201 pS. (*D*) Recordings of the smaller amplitude single-channel currents from an outside-out membrane patch exposed to an asymmetrical K^+ gradient (4.7/135 mM) in the presence of 1 mM TEA in the bath solution. The membrane patch was held at potentials, e.g., 0, +20, and +40 mV, as indicated. (*E*) Single-channel *I–V* curve for data from the small amplitude currents. The slope conductance (g) calculated from the single-channel *I–V* curve was 45 pS.

filled with 135 mM K^+ solution. The bath solution was the same as that used for whole-cell current recording. In cell-attached configuration, the actual patch membrane potential is unknown; however, it is assumed that the patch E_m equals the difference between the pipette command potential and the actual resting E_m (about −40 mV in PASMC). Thus, voltages are expressed as pipette (or applied command) potentials. All experiments were performed at room temperature (22–24°C).

Measurement of $[Ca^{2+}]_i$. The $[Ca^{2+}]_i$ in single PASMC was measured using the fluorescent dye fura-2 and the quantitative fluorescence microscopy system Photoscan M-series (PTI, South Brunswick, NJ). Cells were loaded with the acetoxymethyl ester form of fura-2 (5 μM) as described (15, 27). A single cell of interest was first identified and then illuminated with light from a 75-W xenon lamp. Fura-2 fluorescence (510-nm light emission excited by 340- and 380-nm illumination) from the cell and background fluorescence were measured using a photomultiplier tube via a microscope (Olympus, New Hyde Park, NY; model IMT2) equipped for epifluorescence microscopy. $[Ca^{2+}]_i$ was calculated from the ratio of measured 510-nm fluorescence signals elicited at 340 and 380 nm (15, 27).

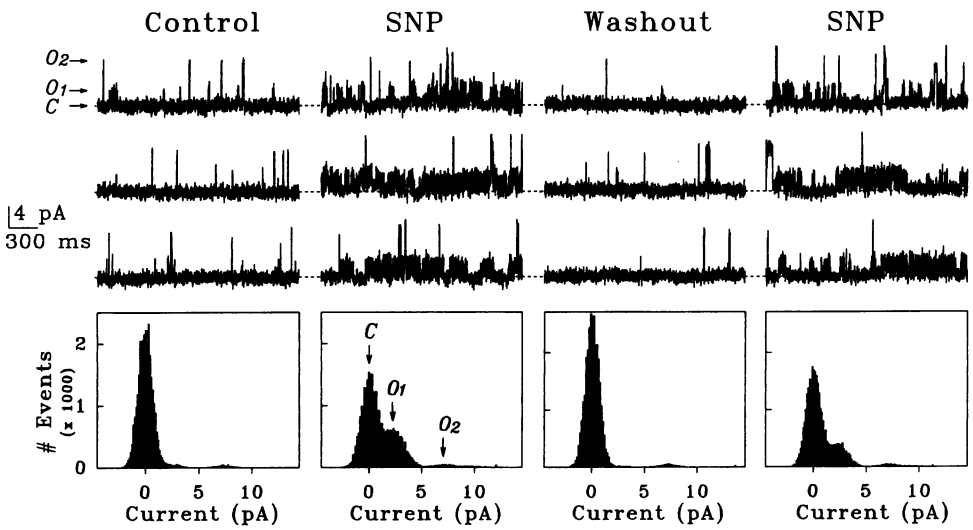

FIG. 3. Effects of SNP on single-channel I_K in excised outside-out membrane patches from PASMC, exposed to an asymmetrical K^+ gradient (4.7 mM/135 mM). At the top of the figure, currents recorded in a patch before (Control), during (SNP), and after (Washout) the cell was exposed to 5 μM SNP are shown. The membrane patch was held at 0 mV. Current levels when channels were closed ("C") are indicated by horizontal broken lines. Upward deflection represents outward current. All-points amplitude histograms constructed from 30-sec segments of the data illustrated in the upper panels are shown at the bottom of the figure. Under control conditions, the steady-state open probability, $N \times P_{open}$, was 0.0188 for the small amplitude I_K, $I_{K(V)}$ (mean unitary current at 0 mV was 2.21 pA, indicated by "O_1"), and 0.0185 for the large amplitude I_K, $I_{K(Ca)}$ (mean unitary current at 0 mV was 7.05 pA, indicated by "O_2"). Upon application of SNP, $N \times P_{open}$ for $I_{K(V)}$ and $I_{K(Ca)}$ were increased to 0.1062 and 0.0332, respectively. The effect was reversed after washout of SNP ($N \times P_{open}$ for $I_{K(V)}$ and $I_{K(Ca)}$ decreased to 0.0144 and 0.0225, respectively). The effect of SNP was also repeatable; re-introduction of SNP to the membrane patch increased $N \times P_{open}$ for $I_{K(V)}$ and $I_{K(Ca)}$ to 0.1220 and 0.0286, respectively.

Tension Measurement of Arterial Rings. Isometric tension was measured in rings obtained from 2nd or 4th order PA branches from Sprague–Dawley rats (150–250 mg) as described (23). Stainless steel wire hooks were used to attach the PA rings to the base of the tissue bath and to the tension transducer. Isometric tension was continuously monitored and recorded on a strip-chart recorder (Linseis, Princeton Junction, NJ), while the tissue was superfused at a rate of 2.5 ml/min with 37°C fluid.

Reagents and Solutions. The standard extracellular physiological salt solution (PSS) used for measuring I_K, $[Ca^{2+}]_i$, and PA tension contained 141 mM NaCl, 4.7 mM KCl, 1.8 mM $CaCl_2$, 1.2 mM $MgCl_2$, 10 mM Hepes, and 10 mM glucose, buffered to pH 7.4 with 5 M NaOH. In Ca^{2+}-free PSS, $CaCl_2$ was replaced by equimolar $MgCl_2$, and 1 mM EGTA was added. The internal (pipette) solution used for recording I_K, in both whole-cell and outside-out configurations, consisted of 125 mM KCl, 4 mM $MgCl_2$, 10 mM Hepes, 10 mM EGTA, and 5 mM Na_2ATP, buffered to pH 7.2 with 1 M KOH.

NO was prepared in double-distilled water at 0°C after deoxygenation by bubbling with 100% N_2 for 60 min. NO gas (>99%; Matheson Gases and Equipment, Baltimore) was then bubbled into 12 ml of water for 20–30 min to produce a saturated NO (≈3 mM at 0°C) stock solution. Freshly prepared NO stock solution (20 μl) was added to 20 ml of superfusate just before use to make a final NO concentration of 3 μM. The half-life of NO (1 μM) in normoxic PSS is 500 sec (7). Although, PSS-containing 3 μM NO was quickly superfused to the tissue chamber within 3–5 min, the concentrations of NO applied to cells are actually much less than those initially dissolved (28) and stated in the text. In some experiments, NO was derived from the NO-generating compound sodium nitroprusside (SNP; 5–10 μM; Sigma). SNP, 4-AP (Aldrich), tetraethylammonium chloride (TEA; Fluka) and sodium nitrite ($NaNO_2$, Sigma) were dissolved directly into PSS on the day of use. ChTX (Accurate Chemicals) and glibenclamide (Sigma) were dissolved in distilled water and dimethyl sulfoxide (Sigma) to make stock solutions of 20 μM and 10 mM, and diluted to final concentrations of 20 nM and 10 μM, respectively, in the bath solution. Similar dilution of dimethyl sulfoxide, alone, into PSS was used as a control; it had no effect on I_K, E_m, or $[Ca^{2+}]_i$.

Statistics. Data are expressed as means ± SE. Statistical analysis was performed using the paired or unpaired Student's *t* test, or analysis of variance, as indicated. Differences were considered to be significant when $P < 0.05$.

RESULTS

Inhibition of K_V Channels by 4-AP. Whole-cell K_V currents ($I_{K(V)}$) were isolated by superfusing PASMC with Ca^{2+}-free PSS (with 1 mM EGTA) and with 10 mM EGTA and 5 mM ATP added to the pipette solutions to minimize K_{Ca} current ($I_{K(Ca)}$) and K_{ATP} current. Under this condition, only $I_{K(V)}$ was elicited by depolarizing cells from a holding potential of −70 mV to +80 mV (Fig. 1) (15, 29). 4-AP (5 mM), a blocker of K_V channels, significantly inhibited $I_{K(V)}$ (Fig. 1*A*), whereas ChTX (20 nM), a K_{Ca} channel blocker (Fig. 1*B*), and glibenclamide, a blocker of K_{ATP} channels (15), negligibly affected $I_{K(V)}$. These results demonstrate that the K^+ currents shown in Fig. 1 are primarily due to K^+ efflux through 4-AP-sensitive K_V channels.

In contrast to the inhibitory effect of 4-AP, bath application of 10 μM SNP (Fig. 1*C*) and ≈3 μM exogenous NO (Fig. 1*D*) significantly enhanced $I_{K(V)}$ in PASMC. For example, SNP and NO increased $I_{K(V)}$, elicited by voltage steps of +80 mV, by 41 ± 7% ($n = 5$; $P < 0.01$) and 36 ± 9% ($n = 7$; $P < 0.05$), respectively (Fig. 1 *C*, *D*, and *F*). The augmenting effect of NO on $I_{K(V)}$ was almost abolished by pretreatment with 5 mM 4-AP (Fig. 1 *E* and *F*).

Augmenting Effects of NO on Single-Channel I_K in PASMC. To clarify the nature of the specific K^+ channel that was activated by NO, the effects of NO on single-channel currents were investigated. In some of the cell-attached patches of PASMC membrane, both large amplitude I_K (Fig. 2*A*, ○) and small amplitude I_K (Fig. 2*A*, ■) were evoked by depolarizing the membrane patch to +70 mV. The conductance of the channels that mediate the large amplitude single channel I_K (Fig. 2*B*) in cell-attached patches is ≈201 pS (symmetric K^+ gradient) (Fig. 2*C*); this corresponds to the conductance of the maxi (large conductance) $I_{K(Ca)}$ (1). A low dose of TEA (1 mM) blocked this $I_{K(Ca)}$ (14), but had no effect on the small

amplitude I_K (Fig. 2*D*), as expected for an $I_{K(V)}$ that was sensitive to 4-AP (not shown). The calculated slope conductance (g) of K_V channels from the current–voltage relationship (I–V) curve for $I_{K(V)}$ was 45 pS (Fig. 2*E*); this corresponds to the conductance of $I_{K(V)}$ described in vascular smooth muscle cells (14, 18, 24).

In excised, outside-out membrane patches from PASMC, extracellular application of 5 μM SNP, a NO-generating compound, significantly and reversibly increased the activity of the smaller amplitude I_K, $I_{K(V)}$ (Fig. 3). The mean increase in the steady-state open probability ($N \times P_{open}$) was 6.01 ± 1.54-fold under these conditions. SNP also increased the activity of the large amplitude I_K, $I_{K(Ca)}$, under low $[Ca^{2+}]_i$ conditions (10 mM EGTA present); the mean increase in $N \times P_{open}$ was 1.70 ± 0.39-fold. Other investigators (30, 31) reported that NO (or Sin-1, a NO-generating compound) caused a 2- to 4-fold increase in $N \times P_{open}$ of $I_{K(Ca)}$ in cerebral and aortic smooth muscle cells in the presence of 100–200 nM internal free Ca^{2+}. In all of these experiments, including ours, K_{ATP} current was minimized by the presence of ATP on the intracellular side of the membrane patch (32).

Effects of NO on E_m and $[Ca^{2+}]_i$ in PASMC. Under resting conditions, $I_{K(V)}$ is an important determinant of E_m (16, 17, 24) in PASMC (15). In turn, E_m regulates $[Ca^{2+}]_i$ (15) by controlling the activity of voltage-gated Ca^{2+} channels. Activation of $I_{K(V)}$ should hyperpolarize, whereas inhibition of $I_{K(V)}$ should depolarize PASMC.

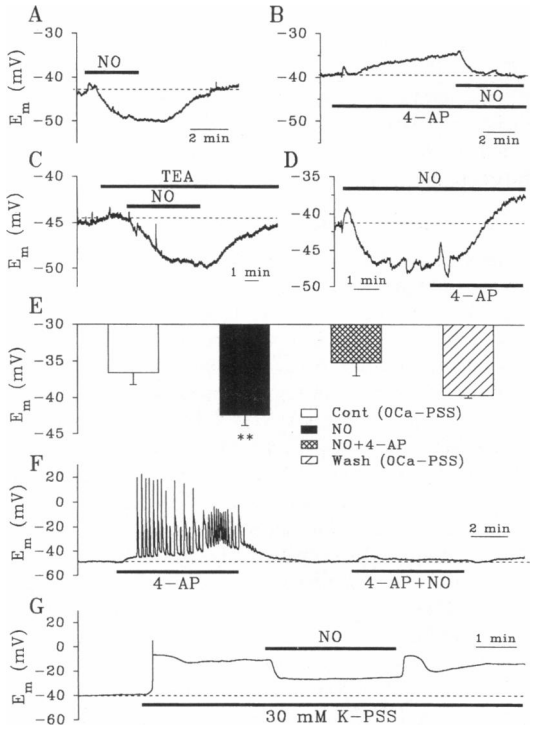

FIG. 4. Effects of authentic NO on E_m in PASMC. (*A*) Effect of ≈3 μM NO on a cell superfused with PSS. (*B*) Effect of NO on a cell treated with 5 mM 4-AP in the absence of extracellular Ca^{2+}. (*C*) Effect of NO on a cell treated with 1 mM TEA. The cell was superfused with Ca^{2+}-containing solution. (*D*) Effect of 4-AP on NO-induced hyperpolarization in the absence of extracellular Ca^{2+}. (*E*) Summary of the effects of NO on E_m in the absence (solid bar) and presence (crosshatched bar) of 4-AP when the cells were superfused with Ca^{2+}-free PSS (0Ca-PSS). Data are means ± SE (n = 5). (*F*) Effect of NO on 4-AP-induced Ca^{2+}-dependent action potentials in the presence of extracellular Ca^{2+}. (*G*) Effect of NO on 30 mM K^+-induced membrane depolarization. At 30 mM, K^+ caused a transient Ca^{2+}-dependent action potential and a steady 30 mV depolarization. NO apparently blocked the Ca^{2+} action potential and caused E_m to decline to E_K, the K^+ equilibrium potential (about −37 mV).

Consistent with its activating effects on $I_{K(V)}$, NO (≈3 μM) reversibly hyperpolarized the PASMC (Fig. 4*A*) from −37 ± 1 mV and −39 ± 1 mV to −43 ± 1 mV (n = 9; $P < 0.001$) and −48 ± 1 mV (n = 6; $P < 0.001$), respectively, in the absence and presence of extracellular Ca^{2+}. NO also blocked 4-AP-induced depolarization (Fig. 4*B*) in the absence of extracellular Ca^{2+}. In either Ca^{2+}-free or Ca^{2+}-containing solutions, the NO-induced hyperpolarization was not affected by 1 mM TEA, which blocks $I_{K(Ca)}$ channels (Fig. 4*C*) but was significantly inhibited by 4-AP, which blocks $I_{K(V)}$ (Fig. 4 *D* and *E*).

In the presence of extracellular Ca^{2+}, inhibition of K_V channels by 4-AP depolarized PASMC to the threshold for activation of voltage-gated Ca^{2+} channels and thereby initiated Ca^{2+} action potentials (Fig. 4*F*). By opening K_V channels (Figs. 1*D* and 3) and antagonizing 4-AP-induced inhibition of K_V channels, NO hyperpolarized PASMC and thereby completely blocked the 4-AP-induced Ca^{2+} action potentials (Fig. 4*F*). Furthermore, NO also reversibly inhibited 30 mM K^+-induced long duration Ca^{2+} action potentials and caused E_m to decline to E_K, K^+ equilibrium potential (about −37 mV) (Fig. 4*G*). The inhibition of Ca^{2+} action potential under these circumstances may be due, at least in part, to direct NO-induced blockade of voltage-gated Ca^{2+} channels (33, 34). Nevertheless, our data imply that NO-induced $I_{K(V)}$ activation is the primary step in this response because the depolarization from the resting E_m, normally required to activate voltage-gated Ca^{2+} channels, is blocked by NO.

Hyperpolarization of PASMC resulting from activation of $I_{K(V)}$ should facilitate closure of voltage-gated Ca^{2+} channels and counteract the depolarization-induced increase in $[Ca^{2+}]_i$. This is illustrated in Fig. 5. Authentic NO (Fig. 5 *A Left* and *B*) and SNP (Fig. 5 *A Right* and *C*) both reversibly inhibited the 4-AP-induced increase in $[Ca^{2+}]_i$. Fig. 5*C* summarizes the inhibitory effect of SNP on the 4-AP-induced increase in $[Ca^{2+}]_i$ in PASMC. In seven PASMC tested, NO (≈3 μM)

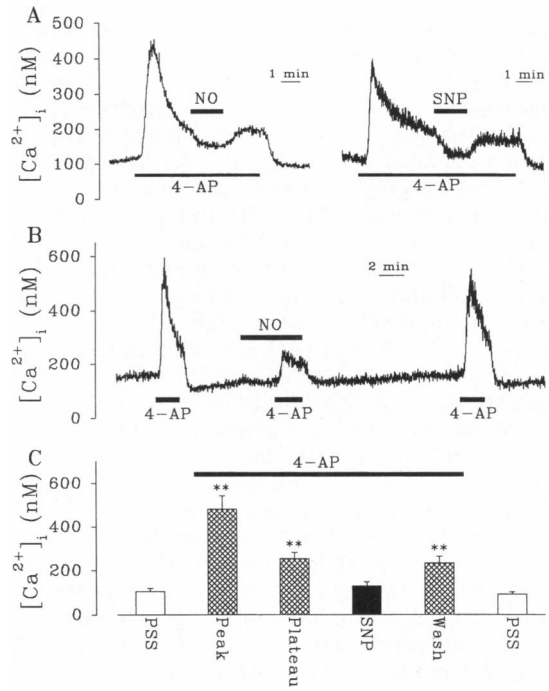

FIG. 5. Inhibitory effects of authentic NO and SNP on $[Ca^{2+}]_i$ in PASMC. (*A*) Representative records illustrate the effects of ≈3 μM NO (*Left*) or 10 μM SNP (*Right*) on 5 mM 4-AP-induced increase in $[Ca^{2+}]_i$. (*B*) NO was applied before introduction of 4-AP. 4-AP-induced increase in $[Ca^{2+}]_i$ was 215 ± 58 nM, 79 ± 22 nM (n = 7; $P < 0.05$), and 169 ± 48 nM before, during, and after introduction of NO, respectively. Cells were superfused with 1.8 mM Ca^{2+}-containing PSS. (*C*) Summary of effects of 4-AP and SNP on $[Ca^{2+}]_i$. Values are means ± SE (n = 20). **, $P < 0.01$ versus control (PSS) and recovery (PSS).

reversibly reduced the 4-AP-induced transient increase in $[Ca^{2+}]_i$ by 63 ± 6% (n = 7; $P < 0.05$).

Effect of 4-AP on NO-Induced Relaxation in Isolated PA Rings. Increasing the extracellular K^+ concentration to 30 mM depolarized PASMC (Fig. 4*G*) and contracted isolated PA rings when external Ca^{2+} was present (Fig. 6). This contraction can be attributed to a rise in $[Ca^{2+}]_i$ due to opening of voltage-gated Ca^{2+} channels and influx of Ca^{2+}. Therefore, as expected for an agent that opens K_V channels and hyperpolarizes PASMC, NO blocked depolarization-induced increase in $[Ca^{2+}]_i$ in single PASMC (Fig. 5) and relaxed the evoked contraction in isolated PA rings (Fig. 6).

Application of 5 mM 4-AP slightly increased 30 mM K^+-induced PA contraction (from 550 ± 58 mg to 597 ± 62 mg; n = 8) but greatly decreased NO-induced PA relaxation (from 43 ± 3% to 24 ± 2%; n = 8) (Fig. 6). These data indicate that NO and 4-AP have opposite effects on K_V channels, E_m, and $[Ca^{2+}]_i$ in PASMC.

The NO-mediated direct blockade of voltage-gated Ca^{2+} channels (33, 34) may also be, at least in part, involved in the relaxant effect of NO on 30 mM K^+-induced PA contraction (Fig. 6). However, nearly half (44 ± 7%) of the NO-induced relaxation is blocked by 4-AP (Fig. 6 *A Right* and *B*). This 4-AP-sensitive portion is likely due to activation of K_V channels and the resultant membrane hyperpolarization.

Effects of $NaNO_2$ on E_m and PA Contraction. The saturated NO stock solution, in addition to containing ≈3 mM NO, also includes about 10 mM nitrite (28). To rule out the possibility that it is the contaminating nitrite in the NO solution, rather than the NO itself, that is responsible for the effects on E_m and PA contractile tone, we tested the effects of sodium nitrite ($NaNO_2$) on E_m and PA contraction. Application of 10 μM $NaNO_2$ negligibly affected either E_m (Fig. 7*A*) or 30 mM K^+-induced PA contraction (Fig. 7 *B* and *C*), whereas addition of ≈3 μM NO (Fig. 7*B*) or 10 μM SNP (Fig. 7*C*) significantly relaxed the PA rings precontracted with 30 mM K^+-containing PSS. More important, whole-cell $I_{K(V)}$ elicited by depolarizing the cells from a holding potential of −70 mV to +80 mV was insignificantly decreased by 10 μM $NaNO_2$ (by 5 ± 4%; n = 8; P = 0.36).

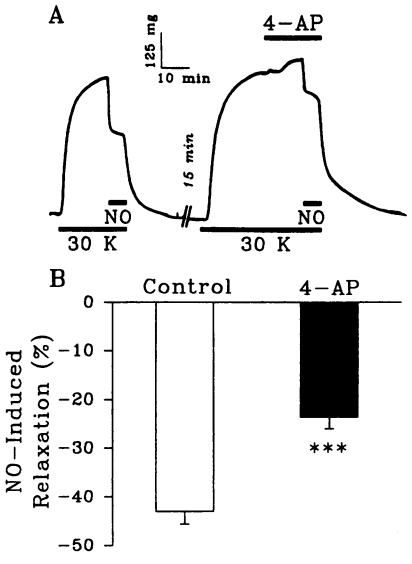

FIG. 6. Inhibitory effect of 4-AP on NO-induced relaxation in isolated PA rings. The ring was equilibrated in PSS for 60 min and contractions were then elicited by 30 mM K^+ (30 K). (*A*) The contracted ring was exposed to ≈3 μM NO, in the absence (*Left*) or presence (*Right*) of 5 mM 4-AP. (*B*) Summary of NO-induced PA relaxation in the absence (open bar) or presence (solid bar) of 4-AP. Values are means ± SE (n = 8). ***, $P < 0.001$ versus control.

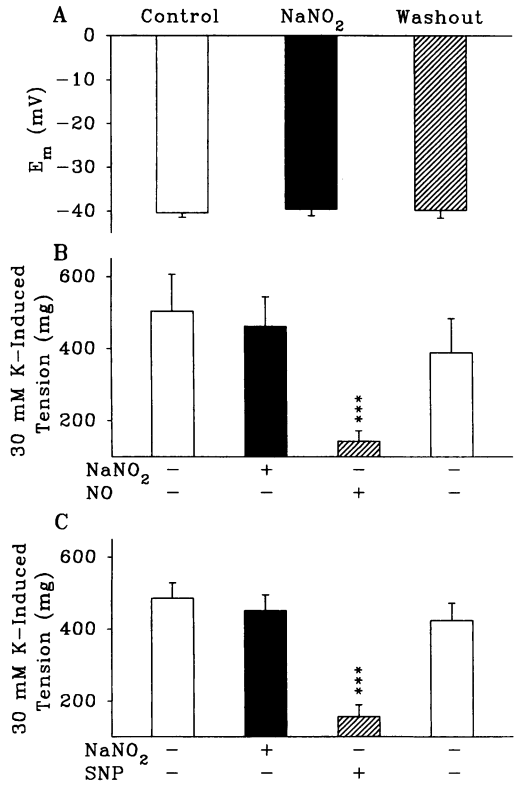

FIG. 7. Effects of $NaNO_2$ on E_m and PA contraction. (*A*) E_m was measured before, during, and after bath application of 10 μM $NaNO_2$. (*B*) 30 mM K^+-induced tension in isolated PA rings was recorded before (open bar) and during application of 10 μM $NaNO_2$ (solid bar) or 3 μM NO (hatched bar; n = 8). (*C*) The 30 mM K^+-induced tension was recorded before (open bar) and during application of 10 μM $NaNO_2$ (solid bar) or 10 μM SNP (hatched bar; n = 6). The PA rings were equilibrated in PSS for 60 min, and contractions were elicited by replacing NaCl with 30 mM KCl in PSS. Values are means ± SE. ***, $P < 0.001$ versus the open and solid bars.

DISCUSSION

Endogenous NO is synthesized from L-arginine by constitutive endothelial NO synthase in vascular endothelium (11). It can also be produced in smooth muscle cells, fibroblasts, and neurons (35). The dependence of the endothelial NO synthase-catalyzed reaction on O_2, NADPH, and Ca^{2+} (11, 35) links NO production in endothelial cells to cellular metabolism, redox status, and Ca^{2+} homeostasis (4, 7, 11). Under normoxic conditions, NO is continuously released into the pulmonary vascular bed (5) and thus plays an important role in regulating basal pulmonary vascular tone (4). Inhaled NO reverses pulmonary vasoconstriction in normal animals and humans as well as in patients with pulmonary hypertension (8, 9).

In vascular smooth muscle, E_m, which is regulated by K^+ channel activity, plays an important role in controlling vasomotor tone and vascular resistance. Inhibition of K^+ channels depolarizes PASMC and consequently increases $[Ca^{2+}]_i$ by activating voltage-gated Ca^{2+} channels. Conversely, activation of K^+ channels hyperpolarizes the cells and, accordingly, decreases $[Ca^{2+}]_i$ by closing voltage-gated Ca^{2+} channels.

The cellular mechanism of NO-mediated regulation of pulmonary vascular tone is poorly understood. The following mechanisms have been proposed to explain the NO-induced pulmonary vasodilation: (*i*) an increase of cellular cGMP content (11), (*ii*) functional alterations of various membrane channels (30, 33, 34, 36), (*iii*) membrane hyperpolarization (12, 13), and (*iv*) stimulation of sarcolemmal and sarcoplasmic reticulum Ca^{2+}-ATPases (10).

This study shows that (*i*) NO increases $I_{K(V)}$ in intact cells and excised membrane patches; (*ii*) NO causes membrane hyperpolarization in PASMC, which can be blocked by 4-AP; (*iii*) NO prevents 4-AP-induced membrane depolarization and Ca^{2+}-dependent action potentials; (*iv*) NO inhibits 4-AP-induced increases in $[Ca^{2+}]_i$; and (*v*) NO-induced relaxation in isolated PA rings is greatly diminished by 4-AP. These data are all consistent with the idea that the PA endothelium can regulate pulmonary vascular tone by NO-induced functional changes in the PASMC K_V channels that are active under physiological conditions (15).

Role of K_V Channels in Regulating E_m and $[Ca^{2+}]_i$ in PASMC. At least three classes of K^+ channels (14) have been recognized in PASMC: K_V channels (*A*-type, delayed rectifier, and noninactivating components) (15, 24, 37), K_{ATP} channels (14, 38), and K_{Ca} channels (39). Smooth muscle cells undergo phenotypic changes in culture; nevertheless, primary cultured PASMC appear to have the same fundamental mechanisms as do PASMC *in situ* in terms of electrophysiological properties (i.e., K^+, Ca^{2+}, and Cl^- currents), intracellular Ca^{2+} homeostasis, and responses to hypoxia (40). Resting $[Ca^{2+}]_i$ in PASMC ranges from 50 nM to 200 nM, and most K_{Ca} channels are closed (at <0 mV) when $[Ca^{2+}]_i$ is ≤300 nM (39). Thus, under resting conditions, in which $[Ca^{2+}]_i$ is ≈100 nM and E_m is −55 to −35 mV (14), K_{Ca} channels are largely inactive. Furthermore, the intracellular ATP level is in the range of 1–3 mM (32), and K_{ATP} channels are completely blocked by ≈3 mM ATP (14, 32, 38). Hence, most K_{ATP} channels are also closed under normoxic and physiological conditions.

On the other hand, a significant fraction of the K_V channels are open in resting PA myocytes, and these channels appear to be a major contributor to the regulation of resting E_m (15–17, 22, 24, 41) and, consequently, $[Ca^{2+}]_i$ in PASMC (15). Participation of K_{Ca} and K_{ATP} channels in the regulation of E_m and $[Ca^{2+}]_i$, under conditions in which $[Ca^{2+}]_i$ is increased or cellular metabolism is reduced, provides important negative feedback pathways to control vascular tone and stimulation-induced active tension in the pulmonary vasculature.

Effects of NO on K^+ Channels Other than K_V Channels. In addition to the activation of K_V channels, shown in this study, NO also activates K_{Ca} channels (30, 36), K_{ATP} channels (42), and inwardly rectifying K^+ channels (43), and inhibits Ca^{2+} channels (33, 34). Archer and coworkers (36) reported that NO-elicited augmentation of K_{Ca} channels in rat PASMC is due to a soluble guanylate cyclase-induced increase in cGMP production. The resulting phosphorylation, induced by cGMP-dependent protein kinase, augments $I_{K(Ca)}$. In contrast, other investigators (30, 44) have concluded that NO directly augments $I_{K(Ca)}$ by a mechanism that is independent of guanylate cyclase and cGMP. In our study, NO (or SNP) consistently activated $I_{K(V)}$ in both whole-cell (Fig. 1) and excised patch (Fig. 3) configurations. The latter observation suggests that NO may affect K_V channels in rat PASMC directly, without the intervention of soluble guanylate cyclase.

The fact that 4-AP incompletely reversed the NO-induced relaxation in isolated PA rings suggests that the activation of K_V channels is not the only mechanism responsible for NO-induced relaxation. Indeed, redundancy of mechanisms may be a safety factor. Nevertheless, our data demonstrate that modulation of K_V channels contributes significantly to the mechanisms by which NO hyperpolarizes and relaxes the pulmonary vasculature.

Conclusion. In sum, our results show that NO, a potent endothelium-derived relaxing factor, directly activates 4-AP-sensitive K_V channels in PASMC. The consequent membrane hyperpolarization and decrease in $[Ca^{2+}]_i$, at least in part, contribute to the NO-induced relaxation response in pulmonary arteries under physiological and pathological conditions. This may explain why NO is an effective therapeutic agent in cases of pulmonary hypertension and other diseases associated with excessive pulmonary vasoconstriction.

We thank A. M. Aldinger, Y. Zhao, and J. Wang for their excellent technical assistance. This work was supported by National Institutes of Health Grants HL-54043 (X.-J.Y.), HL-43304 (M.L.T.), HL-02659 (L.J.R.), and HL-32276 (M.P.B.) and a grant from the American Heart Association—Maryland Affiliate (X.-J.Y.). X.-J.Y. is a Parker B. Francis Fellow in Pulmonary Research and a recipient of the Giles F. Filley Memorial Award from the American Physiological Society. M.L.T. is an Established Investigator of the American Heart Association.

1. Furchgott, R. F. & Zawadzki, J. V. (1980) *Nature (London)* **288,** 373–376.
2. Ignarro, L. J., Buga, G. M., Wood, K. S., Byrns, R. E. & Chaudhuri, G. (1987) *Proc. Natl. Acad. Sci. USA* **84,** 9265–9269.
3. Palmer, R. M. J., Ferrige, A. G. & Moncada, S. (1987) *Nature (London)* **327,** 524–526.
4. Stamler, J. S., Loh, E., Roddy, M.-A., Currie, K. E. & Creager, M. A. (1994) *Circulation* **89,** 2035–2040.
5. Cremona, G., Wood, A. M., Hall, L. W., Bower, E. A. & Higenbottam, T. (1994) *J. Physiol. (London)* **481,** 185–195.
6. Rubanyi, G. M. (1991) in *Cardiovascular Significance of Endothelium-Derived Vasoactive Factors*, ed. Rubanyi, G. M. (Futura, New York), pp. 11–14.
7. Zapol, W. M., Rimar, S., Gillis, N., Marletta, M. & Bosken, C. W. (1994) *Am. J. Respir. Crit. Care Med.* **149,** 1375–1380.
8. Frostell, C. G., Blomqvist, H., Hedenstierna, G., Lundberg, J. & Zapol, W. M. (1993) *Anesthesiology* **78,** 413–416.
9. Pepke-Zaba, J., Higenbottam, T. W., Dinh-Xuan, A. T., Stone, D. & Wallwork, J. (1991) *Lancet* **338,** 1173–1174.
10. Lincoln, T. M. & Cornwell, T. L. (1993) *FASEB J.* **7,** 328–338.
11. Moncada, S., Palmer, R. M. J. & Higgs, E. A. (1991) *Pharmacol. Rev.* **43,** 109–142.
12. Nagao, T. & Vanhoutte, P. M. (1993) *Am. J. Respir. Cell Mol. Biol.* **8,** 1–6.
13. Tare, M., Parkington, H. C., Coleman, H. A., Neild, T. O. & Dusting, G. J. (1990) *Nature (London)* **346,** 69–71.
14. Nelson, M. T. & Quayle, J. M. (1995) *Am. J. Physiol.* **268,** C799–C822.
15. Yuan, X.-J. (1995) *Circ. Res.* **77,** 370–378.
16. Fleischmann, B. K., Washabau, R. J. & Kotlikoff, M. I. (1993) *J. Physiol. (London)* **469,** 625–638.
17. Robertson, B. E. & Nelson, M. T. (1994) *Am. J. Physiol.* **267,** C1589–C1597.
18. Post, J. M., Gelband, C. H. & Hume, J. R. (1995) *Circ. Res.* **77,** 131–139.
19. Yuan, X.-J., Goldman, W. F., Tod, M. L., Rubin, L. J. & Blaustein, M. P. (1993) *Am. J. Physiol.* **264,** L116–L123.
20. Yuan, X.-J., Tod, M. L., Rubin, L. J. & Blaustein, M. P. (1994) *Am. J. Physiol.* **259,** L52–L63.
21. Cornfield, D. N., Stevens, T., McMurtry, I. F., Abman, S. H. & Rodman, D. M. (1993) *Am. J. Physiol.* **265,** L53–L56.
22. Smirnov, S. V., Robertson, T. P., Award, J. P. T. & Aaronson, P. I. (1994) *Am. J. Physiol.* **266,** H365–H370.
23. Yuan, X.-J., Tod, M. L., Rubin, L. J. & Blaustein, M. P. (1990) *Am. J. Physiol.* **259,** H281–H289.
24. Gelband, C. G. & Hume, J. R. (1995) *Circ. Res.* **77,** 121–130.
25. Yuan, X.-J., Goldman, W. F., Tod, M. L., Rubin, L. J. & Blaustein, M. P. (1993) *Am. J. Physiol.* **264,** L107–L115.
26. Hamill, O. P., Marty, A., Neher, E., Sakmann, B. & Sigworth, F. J. (1981) *Pfluegers Arch.* **391,** 85–100.
27. Goldman, W. F., Bova, S. & Blaustein, M. P. (1990) *Cell Calcium* **11,** 221–231.
28. Furchgott, R. F., Khan, M. T. & Jothianandan, D. (1991) in *Endothelium-Derived Relaxing Factors*, ed. Rubanyi, G. M. & Vanhoutte, P. M. (Karger, Basel), pp. 8–21.
29. Volk, K. A., Matsuda, J. J. & Shibata E. F. (1991) *J. Physiol. (London)* **439,** 751–768.
30. Bolotina, V. M., Najibi, S., Palacino, J. J., Pagano, P. J. & Cohen, R. A. (1994) *Nature (London)* **368,** 850–853.
31. Robertson, B. E., Schubert, R., Hescheler, J. & Nelson, M. T. (1993) *Am. J. Physiol.* **265,** C299–C303.
32. Davies, N. W., Standen, N. B. & Stanfield, P. R. (1991) *J. Bioenerget. Biomembr.* **23,** 509–536.
33. Blatter, L. A. & Wier, W. G. (1995) *Cell Calcium* **15,** 122–131.
34. Clapp, L. H. & Gurney, A. M. (1991) *Pfluegers Arch.* **418,** 462–470.
35. Gaston, B., Drazen, J. M., Loscalzo, J. & Stamler, J. S. (1994) *Am. J. Respir. Crit. Care Med.* **149,** 538–551.
36. Archer, S. L., Huang, J. M. C., Hampl, V., Nelson, D. P., Shultz, P. J. & Weir, E. K. (1994) *Proc. Natl. Acad. Sci. USA* **91,** 7583–7587.
37. Smirnov, S. V. & Aaronson, P. I. (1994) *J. Gen. Physiol.* **104,** 241–264.
38. Clapp, L. H. & Gurney, A. M. (1992) *Am. J. Physiol.* **262,** H916–H920.
39. Albarwani, S., Robertson, B. E., Nye, P. C. G. & Kozlowski, R. Z. (1994) *Pfluegers Arch.* **428,** 446–454.
40. Murray, T. R., Chen, L., Marshall, B. E. & Macarak, E. J. (1991) *Am. J. Respir. Cell Mol. Biol.* **3,** 457–465.
41. Leblanc, N., Wan, X. & Leung, P. M. (1994) *Am. J. Physiol.* **266,** C1523–C1537.
42. Tsuura, Y., Ishida, H., Hayashi, S., Sakamoto, K., Horie, M. & Seino, Y. (1994) *J. Gen. Physiol.* **104,** 1079–1098.
43. Janigro, D., West, G. A., Nguyen, T.-S. & Winn, H. R. (1994) *Circ. Res.* **75,** 528–538.
44. Meisheri, K. D., Cipkus-Dubray, L. A., Hosner, J. M. & Khan, S. A. (1991) *J. Cardiovasc. Pharmacol.* **17,** 903–912.